IL NUOVO CIMENTO **38 C** (2015) 66
DOI 10.1393/ncc/i2015-15066-5

COMMUNICATIONS: SIF Congress 2014

Study of the evaporative decay of excited ^{88}Mo nuclei produced in almost mass-symmetric reactions at 6–12 MeV/amu

S. VALDRÉ(*)
Università di Firenze and INFN, Sezione di Firenze - Sesto Fiorentino, (Fi) Italy

received 15 May 2015

Summary. — Medium-mass nuclei ($A \approx 100$) are predicted to be candidates for shape phase transitions at high spin. Experimental studies on their decay are however rather scarce in the literature. In this work some results on the characteristics of charged species emitted by excited ^{88}Mo compound nuclei produced in the reaction ^{48}Ti $+^{40}$ Ca are presented. Three bombarding energies were measured, 300, 450, 600 MeV, in order to better follow the evolution of the fusion-evaporation and fusion-fission channels. The experiment was carried out with a setup featuring an efficient detector for charged products coupled to a BaF_2 scintillator array for hard photons. In this paper we only deal with charged products, neglecting the coincident gamma ray events elsewhere described. Experimental data have been compared with the prediction of the statistical model in its implementation in the GEMINI++ code, well suited even for high spin systems.

PACS 25.70.Gh – Compound nucleus.
PACS 25.70.Jj – Fusion and fusion-fission reactions.
PACS 24.60.Dr – Statistical compound-nucleus reactions.

1. – Introduction

Recent interest rose for the study of excited medium-mass nuclei because they are good candidates for shape transitions induced by very high spin values [1, 2]. Indeed, these nuclei present sizeable fission barriers even at high rotational energies so that the evolution from spherical shapes to prolate or pear-like can be followed up to high spins with scarce competition with fission. A possible signature of such transitions can be found looking at the multimodal behaviour of the GDR energy spectrum, observed at different gates on the nuclear spin. This kind of investigation calls for severe constraints on the statistical models, used to describe at the best the characteristics of the decaying nuclei. In particular, statistical description must be able to describe the decay of these nuclei in an extended range of energies and spins, both for the fusion evaporation and

(*) E-mail: valdre@fi.infn.it

the fission channel. A satisfactorily description of the system properties is needed to estimate the gamma ray background on top of which the GDR appears (at around 10–15 MeV energy) and also for the light particle evaporation; indeed, their features, if sufficiently under control, can be used to put gates on the spin of the decaying system.

Complete measurements on fusion-like reactions, including the coincident detection of evaporation residues (ER) together with light charged particles (LCP) are scarce for this medium-mass nuclear region. Among the available data in literature we can cite, for example [3, 4], where the inclusive decay of ^{67}Ga is investigated at 1.4 AMeV and 1.9 AMeV excitation energy, respectively. In [5] protons and α-particles have been measured in coincidence with ER for the reaction $^{32}\mathrm{S} + ^{74}$ Ge at different beam energies in the range 5–13 AMeV. Also in [6] α-particle energy spectra coming from the decay of ^{56}Ni have been studied in coincidence with the evaporation residue. The main difference between our system and the previously cited ones is that in our case we can have fusion-evaporation reactions with very high values of spin (up to 64 $\hbar$), because of the mass symmetric reaction and the high fission barrier of ^{88}Mo. This characteristics make our system a good benchmark to test the goodness of the statistical model for high-spin and medium-mass compound nuclei.

Statistical models are commonly used to describe the decay of excited nuclei and make indeed a very good job, on average, when applied to reproduce the evaporation spectra of light charged particles or the relative abundances of the various species. However, the details of these emissions are not always constrained and this occurs in particular for medium-mass nuclei. As pointed out in [7], for instance, this can be due to the insufficient knowledge of some relevant ingredients such as the level density parameter or to intrinsic model limitations (*e.g.* the "ad hoc" inclusion of some deformation effects on model parameters).

All above considered, our group undertook an experimental campaign to study the collective γ-ray emissions at high spin values, investigating meanwhile the decay features of these highly excited rotating systems, thus better constraining some key model parameters in this region of the nuclide chart.

2. – The experiment

2˙1. *Reaction characteristics.* – The main reaction parameters for the investigated systems are reported in table I. Looking at the values of the grazing angular momenta (from 91$\hbar$ to 149$\hbar$) compared to the critical ones, we see that for this rather light system, only at the lowest energy the fusion cross section is the dominating reaction mechanism; the nuclear fusion is then followed either by evaporation (FE) or by fission (FF) of the CN. If complete fusion takes place, ^{88}Mo CN are formed with an excitation energy that goes from $E^* = 124$ MeV at 300 MeV beam energy to $E^* = 260$ MeV at 600 MeV beam energy. The angular momentum $l^{\mathrm{f}}_{\mathrm{crit}}$ for which the fission barrier for ^{88}Mo nuclei vanishes is another important parameter in this work; it results $l^{\mathrm{f}}_{\mathrm{crit}} = 64\hbar$ according to Sierk model [8]. However, the compound nucleus formation is possible up to $l_{\max} = 76$–$82\,\hbar$ according to the Bass model [9].

Considering the reaction cross sections, we note that at the highest energy of 600 MeV, there is room for a sizeable contribution of deep-inelastic reactions, producing a quasi-projectile (QP) and a quasi-target (QT) pair. Also, quasi-fusion and quasi-fission modes can be present. All these latter mechanisms populate phase-space regions quite overlapping with those of the fusion-fission channel, which is therefore difficult to be precisely selected.

TABLE I. – *The table displays the following quantities: the projectile kinetic energy, the grazing angle and angular momentum, the maximum value of angular momentum at which is possible to form a compound nucleus, the excitation energy of the compound nucleus* ($E^*_{\rm CN} = E^{(\rm cm)} + Q$) *and the predicted reaction cross sections using Gupta model.*

$E_{\rm b}$ [MeV]	$\vartheta_{\rm gr}$ [°]	$l_{\rm gr}$ [$\hbar$]	$l_{\rm max}$ [$\hbar$]	$E^*_{\rm CN}$ [MeV]	$\sigma_{\rm R}$ [mb]
300	15.8	91	76	124.1	1863
450	9.5	124	82	192.4	2268
600	6.9	149	82	260.4	2446

2˙2. *Experimental apparatus*. – The experiments have been carried out at the INFN *Laboratori Nazionali di Legnaro* (LNL, Italy). Pulsed beams of ^{48}Ti at the three bombarding energies (300, 450, 600 MeV) impinged on a metallic ^{40}Ca target (500 μg/cm^2 thickness) sandwiched between two very thin plastic foils (15 μg/cm^2) against prompt oxidation. Typical beam currents of 0.5–1 pnA were used. In order to study the GDR evolution with excitation energy and spin, a composite apparatus was used. A group of 8 BaF_2 scintillators (HECTOR setup [10-13]) for gamma rays, covering backward laboratory angles, was coupled with our large-acceptance detector for charged reaction products (fig. 1). Here we describe only this latter part of the setup.

The heavy products, in particular evaporation residues from the fusion reactions, were detected by an array of 32 triple-phoswiches of the FIASCO setup [14] mounted in four matrices, each with eight detectors, in an axially symmetric configuration around the beam direction. The phowiches featured two plastic layers (180 μm fast and 5 mm mid-fast scintillators) followed by a CsI(Tl) crystal 4 cm thick, thus presenting a wide dynamic range for pulse shape analysis. These detectors have been equipped with digital electronics [15], purposely developed by the collaboration. This way, the anode pulse waveform were digitized and then the relevant information (time mark, pulse shape and energy-related variables) could be extracted [16]. In practice, for each phoswich one

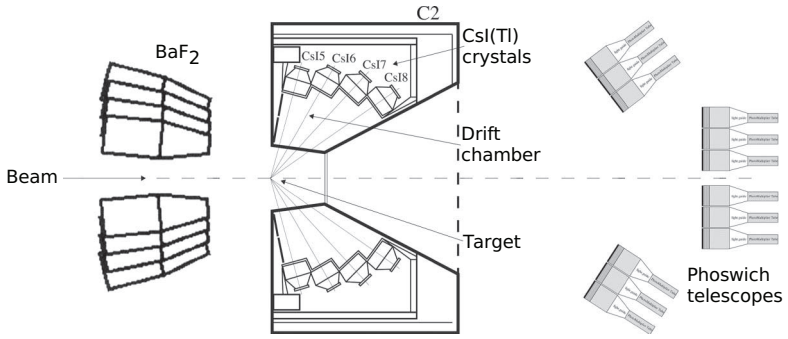

Fig. 1. – The experimental apparatus: to the left side of the picture, at backward angles with respect to the beam, there are 8 BaF_2 scintillators from HECTOR setup. All around the target, between 29.5° and 83° there is the forward chamber of GARFIELD. At forward angles, there are 50 triple-phoswich telescopes from the FIASCO setup.

obtains, besides the time-of-flight (tof), three energy-related variables (gateA, gateB and gateC) roughly corresponding to the energy deposited in the three different active layers. The phoswiches covered the polar region from around 5° to 13° with a significant efficiency for ER detection. Thanks to the first fast plastic layer and to the large distance from the target (1.6 m), the phoswiches permitted good velocity measurement for most ejectiles from $Z = 1$ up to the ER. Charge separation (up to around 16–18) has been obtained with digital pulse shape analysis for particles punching through the thin plastic layer. For $Z = 1$ also the isotopic identification was available via CsI(Tl) pulse-shape analysis. Heavy fusion residues and heavy fission fragments, stopped in the first plastic layer, were detected without charge identification.

The light charged particles and other fragments emitted from the CN decay were measured in the forward chamber of GARFIELD [17], covering polar angles between 29.5° and 83°. GARFIELD is composed of 192 ΔE(gas)-E(CsI(Tl)) modules, equipped with digital electronics and its features and performance are extensively described elsewhere [17, 16]. The thin strip anodes of the ΔE stage provide a moderate gas multiplication while preserving the linear response with energy; thus the internal gain allows for detection and identification from light charged particles to intermediate-mass fragments (typically $Z \approx 10$–12). The 192 modules are organized in four polar rings; each ring consists of 48 effective sectors, with an azimuthal granularity of 7.5°. In this experiment the mechanical constraints related to the mounting of the big BaF_2 crystals imposed a change in the target holder position. As a result the backward rings of GARFIELD were affected by the target shadowing and have been discarded in the present analysis.

The energy calibration of the ΔE-E modules has been performed with specific low energy beams. The overall uncertainty on the measured energy is ≈ 5–6%. For kinematic reasons, heavy residues cannot reach the angles of the GARFIELD setup; as a consequence, GARFIELD was able to identify (and measure the energy) all the charged products of the considered reactions which hit its active surface.

Absolute cross section normalization has been obtained from elastically scattered Ti ions detected via a small plastic scintillator located at $\vartheta \approx 2°$, well below the laboratory grazing angle for all the investigated reactions.

2˙3. *Event selection.* – A first event selection has been done on the trigger level, based on the coincidence of a hit in a phoswich and of a hit in GARFIELD. Considering the geometry of the phoswich wall and the coverage of GARFIELD, this condition strongly selected fusion-evaporation events. To further suppress not interesting events (*i.e.* spurious elastic scattering and binary processes) a level window condition was applied and the trigger fired only for signals above noise but below a given upper threshold imposed on the gateA. In fig. 2 we show a typical *gateA-vs.-tof* correlation, upon which the event selection is mainly based. The plot refers to the reaction at 450 MeV. Fusion-evaporation events are identified by requiring that only one heavy fragment in the phoswich wall be inside the dashed line areal gate traced in the figure. Since, as said, these fragments are stopped in the first thin plastic, charge discrimination of the heavy product is not possible. In the same figure it is clearly visible the yield drop above the upper trigger level. The island of events at high gateA values corresponds to residual elastic scattered ions and has been used for tof calibration.

The fission process for nuclei with $A \approx 100$, below the Businaro-Gallone point, mainly produces two fragments with different sizes. Therefore we expect that in our system the asymmetric splits prevail on the less probable symmetric fissions, as reported in [18] for molybdenum isotopes. Candidates for fission events have been selected on the basis

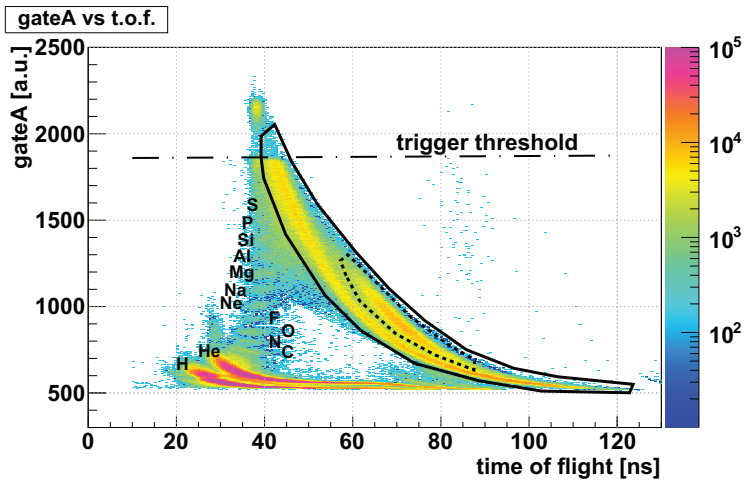

Fig. 2. – Correlation between gateA (see text) and the time of flight for a phoswich telescope at 450 MeV bombarding energy. Areal gates for particle identification are shown: the contour for heavy-fragment selection with a solid line, the contour for evaporation residue selection with dashed line.

of the coincidence of two heavy fragments in the phoswich wall or one in the wall accompanied by an intermediate fragment in GARFIELD. In this latter case asymmetric fissions are automatically chosen for kinematic reasons, the lighter ejectile being detected in GARFIELD. When both fission fragments are detected in the phoswiches, only for sufficiently asymmetric splits charge identification is performed for the lighter partner. The selection gate for the heavier fission fragments is shown again in fig. 2 with a solid line contour.

3. – Experimental results

The results shown in this work have been compared with statistical model calculations in the version of the GEMINI++ code, one of the most acknowledged implementations in the literature. The code is a Monte Carlo package which allows us for creating millions of events corresponding to the decay of excited ^{88}Mo nuclei. These events are then filtered through an accurate software replica of our composite set-up so that the measured distributions and quantities can be directly compared to the simulated ones. Also, the simulations permit to estimate the efficiencies needed to pass from measured quantities (for example LCP multiplicities or fragment yields) to 4π values. Finally, of course, from the quality of the agreement between measured and simulated distributions we can learn about the key model parameters and we can constraint their values.

The fusion-evaporation channel is expected to dominate at the lowest measured beam energy of 300 MeV with scarce, if any, pre-equilibrium contribution, Therefore the lowest energy data set can be considered as a reference case for this channel. By GEMINI simulations at 300 MeV (fig. 3) we estimated that the efficiency for this kind of decay channel is around 10% overall, while it rises to about 40% restricting the ER to emission angles from 5° and 13° which is the region covered by the phoswich wall. At 450 and 600 MeV the efficiency of evaporation residue detection is slightly higher due to the wider angular distribution that covers in a better way the phoswich angular acceptance.

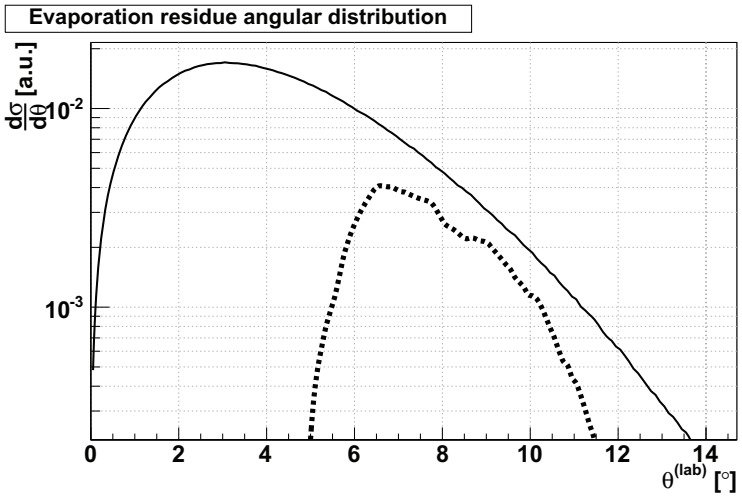

Fig. 3. – GEMINI++ simulation of the evaporation residue angular distribution at 300 MeV. With a solid line the original Monte Carlo distribution is shown. With a dashed line the Monte Carlo distribution corrected with a geometrical and efficiency filter is shown.

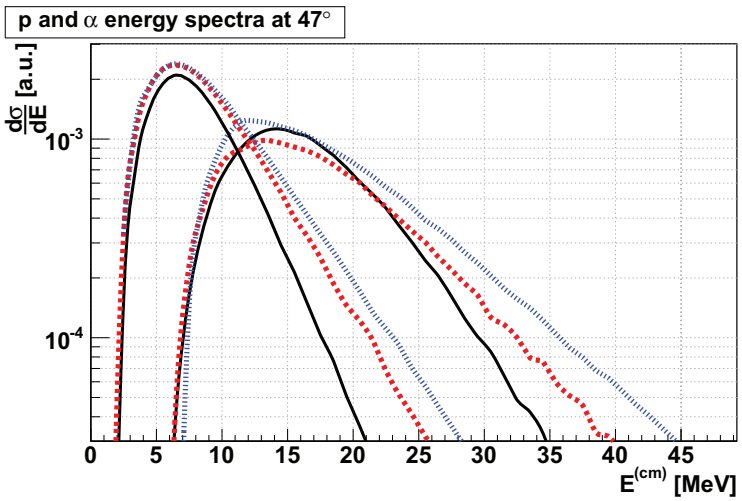

Fig. 4. – Experimental proton and α-particle energy spectra. Higher-energy distributions are referred to α-particles. With a solid black line, a red dashed line and a blue dotted line the 300, 450 and 600 MeV bombarding energy spectra are, respectively, shown.

The LCP multiplicity and energy distributions are key observables to investigate the source characteristics. We found, as expected, that proton and alpha emissions mostly contribute to the measured LCP. Moreover, the abundances of LCP are assumed to grow with increasing beam energy, as the consequence of the increase of the source excitation energy. The experimental centre-of-mass energy distributions (log scale) are shown in fig. 4 for protons and α-particles at the three bombarding energies. The distributions, referring to the GARFIELD ring from 41° to 52°, are normalized to the number of ER for each beam energy. The spectra are typically Maxwellian-like as expected for the evaporation from a hot nuclear source. For both particle types, we clearly observe

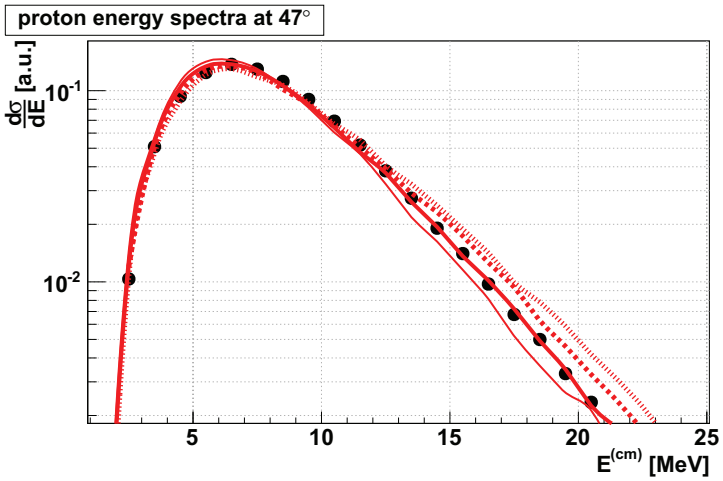

Fig. 5. – Experimental proton energy spectra (full black circles) along with GEMINI++ simulations (red lines) run with different level density parameter $a = A/K$. Thin solid line: $K = 6.0\,\mathrm{MeV}$; thick solid line: $K = 7.3\,\mathrm{MeV}$ (standard value); dashed line: $K = 8.6\,\mathrm{MeV}$; dotted line: $K = 10.0\,\mathrm{MeV}$.

the increase of the inverse slope (apparent temperature) and of the multiplicity with increasing beam energy.

We now concentrate on the comparison with GEMINI++ calculations run with the standard parameter set suggested in [7]. In fig. 5 centre-of-mass experimental spectra obtained for protons emitted with polar angle between 41° and 52° in coincidence with an evaporation residue are presented as full circles for the reaction at 300 MeV; the superimposed red lines are the result of the GEMINI++ code. The thick solid line is produced using standard parameters, while the other lines are obtained changing the level density parameter. The Monte Carlo simulations are filtered with the geometrical acceptance and efficiency of the setup and the spectra are normalized to the integral.

A substantial agreement among experimental spectra and GEMINI++ simulations is evident from these plots. On the contrary, a completely different situation is observed for the α-particles, as it is evident from fig. 6. In this case the slope of experimental α-particle energy spectra is quite harder with respect to GEMINI++ code run with standard parameters (thin solid red line).

The effect on the α-particles of some important model parameters can be now explored. It is well known that the level density parameter (associated to the *little* $-\,a = 1/K$ coefficient) is one of the crucial statistical model ingredients. The GEMINI++ code offers an average parametrization valid for a wide spectrum of nuclides. However, the CN mass region here considered is just one where the *little* $-\,a$ systematics changes rapidly. We ran simulations using K values from 6.0 to 10.0 MeV, around the default choice in GEMINI++ (7.3 MeV), obtaining that this default value is the one that better reproduces proton experimental data (fig. 5). Unfortunately, varying *little* $-\,a$ values does not significantly affect α-particle energy spectra.

In GEMINI++ Coulomb barrier fluctuations are taken into account in an approximate way. They are somehow mimicked introducing a sum of three barrier heights with a temperature dependent mixing parameter. We run simulations varying the coefficient of this mixing from the standard value $w = 1.0\,\mathrm{fm\,MeV^{-1/2}}$ to 0 and $1.5\,\mathrm{fm\,MeV^{-1/2}}$, but not even this variation permits to reproduce the experimental data.

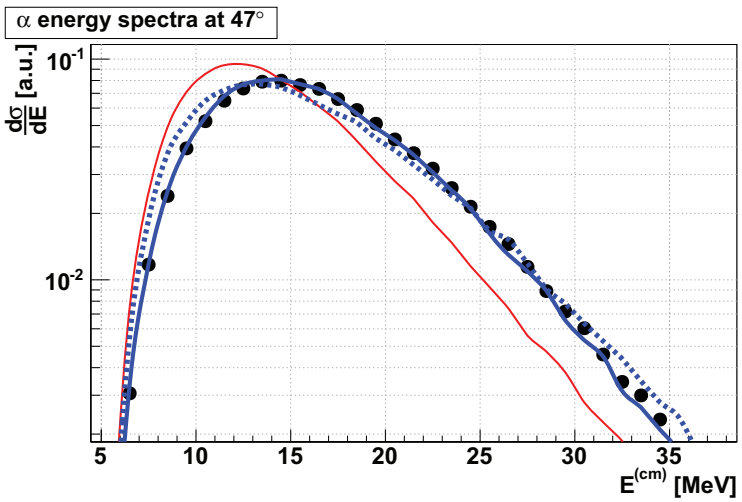

Fig. 6. – Experimental α-particle energy spectra (full black circles) along with GEMINI++ simulations (red and blue lines) run with different Yrast line parametrization and w parameter (see text). Thin solid red line: Sierk model Yrast and fission barrier, $w = 1$ (standard values); dashed blue line: RLDM Yrast and fission barrier, $w = 1$; thick solid blue line: RLDM Yrast and fission barrier, $w = 0$.

Instead, we found that the parametrization of the Yrast line has a strong influence on α-particle emission, while only slightly affects protons. After some attempts we found, according to [19,12,13], that a rather good agreement for the simulated α energy spectra can be found using a RLDM parametrization for Yrast line and fission barriers instead of Sierk ones. Moreover, as noted in the past for similar systems [7], a further improvement is obtained by switching off barrier fluctuations ($w = 0$). The previous comments can be observed in fig. 6

Let us discuss the LCP multiplicities. First we found that the proton multiplicities are faithfully reproduced by GEMINI++ in a way that is almost independent of the parameter set. Instead, as seen in fig. 7, for α-particles we observe a different trend. At the lowest investigated $E_{\rm beam}$ the data are fully compatible with statistical emission, but with increasing energy an enhanced production at forward angles is observed and it cannot be accounted for by GEMINI++, irrespective of the choice of the parameters.

Table II summarizes the multiplicities, measured and simulated. The measured ones have been corrected for the efficiency. Assuming that the α-particle excess is associated to pre-equilibrium emission and observing that GEMINI++ rather correctly reproduces the data at the angles covered by GARFIELD, we estimate the multiplicities also restricting the data only to the LCP detected in GARFIELD. This explains the first two columns. For protons (deuteron and triton statistics is too low and their values are discarded) GEMINI++ follows closely the measured values at the three energies; for α-particles, instead, only if we restrict to GARFIELD the multiplicities are essentially reproduced also at the higher energies. The differences between the values of the two first columns can be interpreted as the onset of new non-statistical processes (maybe pre-equilibrium emission). A more complete discussion on this aspect is out of the scope of this paper. Some details can be found in [20].

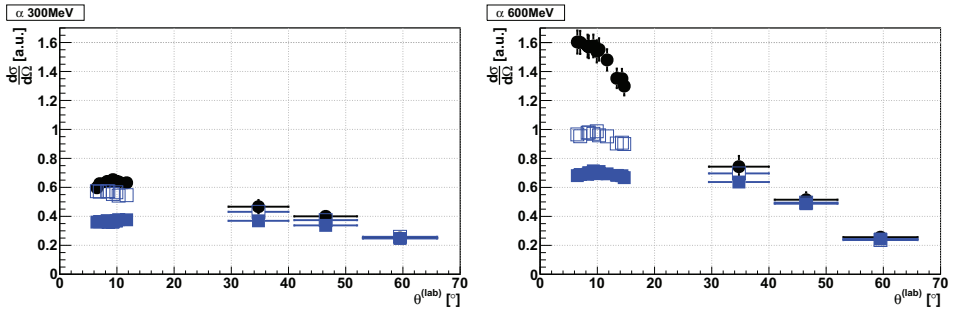

(a) 300 MeV (b) 600 MeV

Fig. 7. – α-particle yield as a function of the lab polar angle. Full black circles: experimental data; open blue squares: GEMINI++ with RLDM Yrast line and fission barrier and $w = 1$; full blue squares: GEMINI++ with RLDM Yrast line and fission barrier and $w = 0$.

4. – Summary and conclusions

In this work we presented some results from the study of the ^{88}Mo compound nucleus decay at three bombarding energies (300, 450 and 600 MeV). Data have been collected by means of the GARFIELD setup coupled to a wall of phoswich telescopes of the FIASCO device.

We have found that at 300 MeV the statistical model reproduces rather well LCP features; for α-particles a tuning of the model parameters has been necessary, suggesting rather spherical configurations for the sources. Instead, with increasing bombarding energies, we observe an excess of α-particle emission which cannot be accounted for by GEMINI++, even exporting the parameter set chosen at 300 MeV. Proton emission is well explained by the model at all the studied energies, provided that the proper parameters have been selected. The clear trend with increasing bombarding energies suggests the onset of some non-statistical emission or spurious contributions from non-fusion reactions (such as quasi-fusion or DIC) which are more abundant and difficult to be clearly separated.

Basing on these findings our group is planning new experiments on similar systems with more powerful detectors at forward angles to better characterize the emission sources.

TABLE II. – *Multiplicities of LCP detected in coincidence with an ER, corrected for the efficiency.*

		Integral data	GARFIELD data	GEMINI++
300 MeV	p	3.72 ± 0.09	3.87 ± 0.05	3.02 ± 0.22
	α	1.76 ± 0.18	1.70 ± 0.22	1.53 ± 0.34
450 MeV	p	4.83 ± 0.15	4.73 ± 0.15	4.42 ± 0.26
	α	2.33 ± 0.12	1.88 ± 0.14	1.93 ± 0.39
600 MeV	p	5.02 ± 0.21	4.64 ± 0.21	5.66 ± 0.25
	α	2.81 ± 0.20	2.24 ± 0.18	2.12 ± 0.34

REFERENCES

[1] Maj A. *et al.*, *Int. J. Mod. Phys. E*, **19** (2010) 532.
[2] Mazurek K. *et al.*, *Acta Phys. Pol. B*, **42** (2011) 471.
[3] La Rana G. *et al.*, *Phys. Rev. C*, **35** (1987) 373.
[4] Brown C. M. *et al.*, *Phys. Rev. C*, **60** (1999) 064612.
[5] Nebbia G. *et al.*, *Nucl. Phys. A*, **578** (1994) 285.
[6] Bhattacharya C. *et al.*, *Phys. Rev. C*, **65** (2001) 014611.
[7] Charity R. J., *Phys. Rev. C*, **82** (2010) 014610.
[8] Sierk A. J., *Phys. Rev. C*, **33** (1986) 2039.
[9] Bass R., *Nucl. Phys. A*, **231** (1974) 45.
[10] `www.mi.infn.it/camera/images/hector_info.htm`.
[11] Maj A. *et al.*, *Nucl. Phys. A*, **571** (1994) 185.
[12] Ciemała M. *et al.*, *EPJ Web of Conferences*, **66** (2014) 02020.
[13] Ciemała M. *et al.*, *Phys. Rev. C*, **91** (2015) 054313.
[14] Bini M. *et al.*, *Nucl. Instrum. Methods A*, **515** (2003) 497.
[15] Pasquali G. *et al.*, *Nucl. Instrum. Methods A*, **570** (2007) 126.
[16] Bruno M. *et al.*, *Eur. Phys. J. A*, **49** (2013) 1.
[17] `www.lnl.infn.it/garfweb/garf/`.
[18] Jing K. *et al.*, *Nucl. Phys. A*, **645** (1999) 203.
[19] Ciemała M., private communication.
[20] Valdré S. *et al.*, to be submitted to *Phys. Rev. C* (2015).